

4-Aminoethylamino-emodin – a novel potent inhibitor of GSK-3 β – acts as an insulin-sensitizer avoiding downstream effects of activated β -catenin

Rolf Gebhardt ^{a, *}, Katja S. Lerche ^a, Frank Götschel ^{b, †}, Robert Günther ^c, Jens Kolander ^d, Lars Teich ^d, Sebastian Zellmer ^a, Hans-Jörg Hofmann ^c, Kurt Eger ^d, Andreas Hecht ^b, Frank Gaunitz ^a

^a Institute of Biochemistry, Medical Faculty, University of Leipzig, Germany

^b Institute of Molecular Medicine and Faculty of Biology, University of Freiburg, Germany

^c Institute of Biochemistry, Faculty of Biosciences, Pharmacy, and Psychology, University of Leipzig, Germany

^d Institute of Pharmacy, Faculty of Biosciences, Pharmacy, and Psychology, University of Leipzig, Germany

Received: December 22, 2008; Accepted: January 28, 2009

Abstract

Glycogen synthase kinase-3 β (GSK-3 β) is a key target and effector of downstream insulin signalling. Using comparative protein kinase assays and molecular docking studies we characterize the emodin-derivative 4-[N-2-(aminoethyl)-amino]-emodin (L4) as a sensitive and potent inhibitor of GSK-3 β with peculiar features. Compound L4 shows a low cytotoxic potential compared to other GSK-3 β inhibitors determined by the 3-[4,5-dimethylthiazol-2-yl]-2,5-diphenyl tetrazolium bromide assay and cellular ATP levels. Physiologically, L4 acts as an insulin-sensitizing agent that is able to enhance hepatocellular glycogen and fatty acid biosynthesis. These functions are particularly stimulated in the presence of elevated concentrations of glucose and in synergy with the hormone action at moderate but not high insulin levels. In contrast to other low molecular weight GSK-3 β inhibitors (SB216763 and LiCl) or Wnt-3 α -conditioned medium, however, L4 does not induce reporter and target genes of activated β -catenin such as TOPflash, Axin2 and glutamine synthetase. Moreover, when present together with SB216763 or LiCl, L4 counteracts expression of TOPflash or induction of glutamine synthetase by these inhibitors. Because L4 slightly activates β -catenin on its own, these results suggest that a downstream molecular step essential for activation of gene transcription by β -catenin is also inhibited by L4. It is concluded that L4 represents a potent insulin-sensitizing agent favouring physiological effects of insulin mediated by GSK-3 β inhibition but avoiding hazardous effects such as activation of β -catenin-dependent gene expression which may lead to aberrant induction of cell proliferation and cancer.

Keywords: 4-aminoethyl-aminoemodin • β -catenin • glycogen synthase kinase-3 β • inhibition • insulin-sensitizer • protein kinase inhibitor • signalling

Introduction

Type 2 or non-insulin-dependent diabetes mellitus (NIDDM) is a common disease and afflicts about 120 million people worldwide. NIDDM accounts for roughly 90% of all cases of diabetes and is

characterized by insulin resistance, *i.e.* the inability of the body to effectively respond to circulating insulin. Key players in insulin signalling pathways that stimulate glycogen synthesis are the protein kinases AKT/PKB (protein kinase B) and glycogen synthase kinase-3 (GSK-3). Activation of AKT/PKB in response to insulin is mediated by phosphatidylinositol 3-kinase together with further kinases, protein kinases D (PKD)-1 and PKD-2 [1, 2]. Active AKT/PKB phosphorylates and, thus, inactivates GSK-3. Consequences of this inactivation may be different for different GSK-3 isozymes and in different tissues such as muscle and liver [3]. Because GSK-3 is responsible for the inactivation of glycogen synthase when this protein is pre-phosphorylated by casein kinase II (CK-2) [4], inactivation of GSK-3 results in the activation of glycogen synthesis.

[†]Present address: German Cancer Research Center (DKFZ), Heidelberg, Germany.

*Correspondence to: Rolf GEBHARDT, Institute of Biochemistry, Medical Faculty, University of Leipzig, Johannisallee 30, 04103 Leipzig, Germany. Tel.: +49-341-9722100 Fax: +49-341-9722109 E-mail: rgebhardt@medizin.uni-leipzig.de

Therefore, inhibitors of GSK-3 should mimic insulin action and result in enhanced glycogen synthesis and in lower plasma glucose levels. This has been shown, for instance, for lithium chloride (LiCl), a well-known inhibitor of GSK-3, which exerts insulin-like effects on glycogen synthesis and glucose uptake in insulin-sensitive tissues [5, 6]. In addition, LiCl reduces expression of glucose-6-phosphatase and phosphoenolpyruvate carboxykinase genes, whose expression is suppressed by insulin [7]. Further orchestration by insulin of glucose and lipid metabolism may occur *via* the transcription factor adipocyte determination- and differentiation-dependent factor 1 (ADD-1)/SREBP-1c whose transcriptional activity is also regulated by GSK-3-dependent phosphorylation [8].

The serine/threonine kinase GSK-3 exists in two isoforms (α and β) with approximately 98% homology at the catalytic domain [9]. Both isoforms are constitutively active in cells, but cannot completely substitute for each other. Besides glycogen synthase, GSK-3 β has a plethora of different targets [10], among them are components of Wnt-, Hedgehog- and other signalling pathways, many transcription factors and proteins involved in regulating apoptosis [11–13]. Another important target of GSK-3 β is the microtubule-associated protein τ [14]. τ -hyperphosphorylation occurs early under neuro-degenerative conditions such as Alzheimer's disease (AD) and is thought to promote microtubule disassembly [14, 15]. GSK-3 β is also involved in the production of amyloid β -peptides [16] and, therefore, is considered to play a decisive role in the pathological process of AD [17, 18]. Thus, the central role of GSK-3 β in distinct cell types and especially in the disorders mentioned above renders this enzyme a promising target for the potential treatment of NIDDM, AD and other diseases [19, 20].

Several groups have reported on small-molecule inhibitors of GSK-3 β (for reviews see [11–13, 21]). Most of these (*e.g.* Ro 31–8220, SB 216763, hymenaldisine, indirubins, aloisines and paullones) have been described as ATP-competitive GSK-3 inhibitors [13] which, in contrast to previous claims of specificity, were recently found to inhibit, at least partially, one or more additional kinases [22]. Though all these inhibitors were shown to exert many insulin-like effects *in vitro* and often also *in vivo*, a common event distinct from normal insulin action which was reported for most of these compounds, is the activation of β -catenin signalling [23–25]. Usually, *i.e.* in the absence of any stimulus (like Wnt-factors), cytoplasmic β -catenin is targeted to proteolytic breakdown by the proteasome (for reviews see [26, 27]). Targeting is initiated by binding to the so-called destruction complex (minimally consisting of Axin, GSK-3 β , adenomatous polyposis coli and CK-1 α) followed by phosphorylation at S45 by CK-1 (priming) and subsequent phosphorylation at residues T41, S37 and S33 by GSK-3 β . Phosphorylated β -catenin is then ubiquitinated and degraded. Inhibition of GSK-3 β , consequently, generates hypophosphorylated β -catenin which can enter the nucleus, heterodimerize with T-cell factor/lymphoid enhancing factor (TCF/LEF) and act as a transcriptional co-activator [28]. Uncontrolled activation of β -catenin was frequently found to be associated with cell proliferation and tumour development [29, 30].

Despite recent progress in understanding insulin signalling, the question of how insulin in the adult organism can act through

inhibition of GSK-3 β , while circumventing activation of β -catenin and hazardous downstream effects thereof, is not yet completely answered. One mechanism described by Cohen's group [31] suggests inhibition of the interaction of GSK-3 with Axin by FRAT-1 (frequently rearranged in advanced T-cell lymphomas 1), which does not interfere with essential cellular functions of GSK-3. Alternatively, functionally distinct pools of GSK-3 may be sequestered from each other by interacting proteins as exemplified by the β -catenin destruction complex [32, 33]. However, it remains unclear whether such mechanisms play a role in the regulation of liver carbohydrate metabolism.

Recently, we have synthesized a panel of new derivatives of emodin, a natural compound occurring in several plants, and evaluated some of their biological effects [34]. Because emodin is a well-known inhibitor of protein kinases including CK-2 [35, 36], we speculated that derivatives of this lead compound might show altered potency and specificity in inhibiting protein kinases and performed a screening using various *in vitro* kinase assays. In this study, we show that one representative of our series of novel emodin derivatives, 4-[N-2-(aminoethyl)-amino]-emodin (L4) (Fig. 1), is a potent inhibitor of GSK-3 β . Using various cellular systems to detect functional consequences of GSK-3 β inhibition, we could demonstrate that compound L4 mimics various aspects of insulin action in an excellent manner, while avoiding transcriptional activation of TCF/LEF target genes *via* activation of β -catenin.

Materials and methods

Materials

Recombinant rat CK-1 δ was purchased from Sigma-Aldrich (Taufkirchen, Germany) and the substrate (RRKDLHDEEDEAMSITA) was obtained from Calbiochem (Merck Biosciences GmbH, Schwalbach, Germany) as was protein kinase CK-2 (human recombinant). The substrate (RRREETEEE) of CK-2 was purchased from Upstate Biotechnology (Lake Placid, NY, USA). Recombinant rabbit GSK-3 β was received from New England Biolabs GmbH (Frankfurt, Germany). The prephosphorylated substrate for GSK-3 β (KRREILSRPS(PO)YR) derived from the phosphorylated form of δ -CREBP was synthesized by Dr. S. Rothmund at the Interdisciplinary Centre for Clinical Research (IZKF), Leipzig.

SB216763 was obtained from Sigma-Aldrich (Taufkirchen, Germany), and 4-benzyl-2-methyl-1,2,4-thiadiazolidine-3,5-dione (TDZD-8) was from Calbiochem. D-[U-¹⁴C]glucose (230 mCi/mmol), uridine bisphospho-D-[6-³H]glucose, ammonium salt (20 Ci/mmol) and [γ -³²P]-ATP (5000 Ci/mmol) were purchased from GE Healthcare, Amersham Bioscience Europe GmbH, Freiburg, Germany.

HepG2 cells were obtained from ATCC (<http://www.lgcpromochem.com/atcc/>). Cell culture material was obtained from TPP (Trasadingen, Switzerland). Dulbecco's modified Eagle's medium (DMEM) and foetal calf serum (FCS) were purchased from PAA Laboratories (Cölbe, Germany).

All other chemicals were of analytical grade and were purchased from Sigma, Merck (Darmstadt, Germany) or Roth (Karlsruhe, Germany).

Chemistry

The synthesis of emodin derivatives by a novel strategy was described previously [34]. The purified compounds were characterized by ^1H and ^{13}C nuclear magnetic resonance spectra obtained with a Varian Gemini-300 spectrometer. Stock solutions of all compounds were prepared at 40mM in dimethyl sulfoxide (DMSO).

Kinase assays

GSK-3 β

GSK-3 β -kinase activity was assayed in a total volume of 20 μl containing 50 mM Tris-HCl, pH 7.4, 5 mM MgCl_2 , 1 mM NaF, 1 mM PMSF, 1 mM Na_3VO_4 , 3.75 μM unlabelled ATP, 0.2 μCi [γ - ^{32}P]-ATP, 2 mg/ml bovine serum albumin and 5 U of GSK-3 β . Pre-incubation was carried out for 10 min. at 30°C. The reaction was then initiated by addition of 20 μM synthetic GSK-3 peptide substrate. Blanks were run without substrate and the DMSO control without inhibitor. Assays were stopped after 10 min. by addition of 90 μl of 10 mM unlabelled ATP and 40 μl aliquots were immediately spotted onto P81 phosphocellulose filters (Whatman GmbH, Dassel, Germany). Filters were dried for 20 min. and washed five times thereafter in 1% phosphoric acid under continuous shaking for 5 min. They were dried again and placed into 5 ml Ultima Gold scintillation cocktail (Canberra-Packard, Frankfurt, Germany) before counting in a liquid scintillation counter (Tri-carb 2500TR).

CK-1 and CK-2 assays

CK-1 phosphorylation assays were carried out in a total volume of 20 μl , containing 25 mM Tris-HCl, pH 7.4, 10 mM MgCl_2 , 3.75 μM unlabelled ATP, 6.8 U CK-1, 2 mg/ml bovine serum albumin and 0.2 μCi [γ - ^{32}P]-ATP according to the Promega protocol of CK-1 (Promega GmbH, Mannheim, Germany). Pre-incubation was carried out for 10 min. at 30°C. The reaction was started by addition of 20 μM synthetic CK-1 peptide substrate. Blanks were run without substrate and the DMSO control without inhibitor. Assays were stopped after 10 min. by addition of 90 μl of 10 mM orthophosphoric acid. Further processing was performed as described above for GSK-3 β .

CK-2 phosphorylation was performed using a protocol similar to that used in the study of Ding *et al.* [37] with a buffer consisting of 100 mM Tris-HCl, pH 7.4, 20 mM MgCl_2 , 100 mM NaCl, 50 mM KCl, 0.1 mM Na_3VO_4 , 3.75 μM unlabelled ATP, 0.2 μCi [γ - ^{32}P]-ATP, 20 μM CK-2 substrate, 2 mg/ml and 0.2 μCi [γ - ^{32}P]-ATP. Kinase reaction was initiated by addition of recombinant enzyme. Further processing was performed as described above for CK-1.

EGF-receptor tyrosine kinase and other kinase assays

Determination of epidermal growth factor receptor (EGFR) tyrosine kinase was performed using an ELISA assay in 96-well format (PRK Assay kit, Sigma) as described recently [38]. EGFR tyrosine kinase (Sigma) was used

at 10 μl /well with an activity of 1 U/well. Percentage kinase activities of 10 further kinases (fibroblast growth factor receptor [FGFR], adenosine monophosphate-activated protein kinase [AMPK], cyclin-dependent kinase [CDK]-2/cyclinA, CDK-3/cyclin E, C-Jun N-terminal kinase [JNK]-3, MAPK-activated protein kinase [MAPKAP-K2], mitogen-activated protein kinase [MAPK]-1, mitogen- and stress-activated protein kinase [MSK]-1, protein kinase C [PKC]- α , PKC- β_2 , listed in Table 2) were measured by the Kinase Profiler (Upstate/Chemicon, Heidelberg, Germany). The concentration of ATP was 10 μM and that of test compounds and inhibitors was 10 μM .

Determination of IC₅₀-values

Eight increasing concentrations of each test compound or inhibitor were measured. The concentration range was determined in preliminary experiments. The inhibition curves were analysed by non-linear regression using the Origin 7.0 basis function Logistic.

Cell cultures

Hepatocyte preparation and cultivation

Hepatocytes were isolated from rat and mouse livers. Sprague–Dawley rats (200–260 g) and C57/Bl6 N mice were bred and maintained at Medizinisch-Experimentelles Zentrum of the University of Leipzig according to local ethical rules for animal care. Isolation of hepatocytes by the collagenase perfusion technique was performed as described by Gebhardt *et al.* [39]. Periportal and pericentral hepatocyte subpopulations were isolated by the digitonin/ collagenase perfusion technique as described [40]. After purification by differential centrifugation, hepatocytes were suspended in culture medium A (Williams Medium E containing 2 mM glutamine and 100 U/ml penicillin/streptomycin) supplemented with 10% FCS and were plated on collagen-coated Petri dishes at a cell density of 125.000 cells/cm². After 2 hrs, the medium was changed to serum-free culture medium A. If necessary, further changes of the culture medium were performed every 24 hrs. Further details of cultivation were described in [41].

HepG2 hepatoblastoma cells were cultured in DMEM (1 \times) medium (Gibco, Eggenstein, Germany) supplemented with 2 mM glutamine, 10% FCS, 40 U/ml streptomycin and 50 U/ml penicillin as described elsewhere [42, 43]. Cells were passaged every week at the time they reached confluency. Stocks were kept frozen in liquid nitrogen. Frozen cells were thawed, cultured for 1 week, and passaged at least once before use. Confluent HepG2 cell cultures were used for all experiments. Cells from the HuH7 cell line received the same medium, except that it contained 1 g/l glucose.

Human 293 embryonic kidney cells (ATCC # CRL-1658) and murine NIH3T3 fibroblasts expressing Wnt-3a [44] were cultured as described [45]. The murine neural stem cell-like cell line C17.2 [46] was kept in DMEM, 10% FCS, 5% horse serum, 2 mM glutamine and 100 U/ml penicillin/streptomycin at 37°C and 5% CO₂. To obtain Wnt-3a-conditioned media, 2.5 \times 10⁵ NIH3T3-Wnt-3a cells were seeded into 75 cm² dishes in 10 ml media. Four days after seeding, the media were collected and replaced by 10 ml of fresh growth media. A second sample of conditioned media was collected 7 days after seeding. Both samples were combined and stored at 4°C until use.

Incubation of hepatocyte cultures with the test compounds and other GSK-3 β inhibitors

In order to screen for possible influences of the test compounds on intact cells, L4 or other inhibitors of GSK-3 β were added to the culture medium 2 or 26 hrs after seeding the hepatocytes. Stock solutions of the test compounds in DMSO were diluted to reach final concentrations of 0.5 μ M up to 200 μ M. DMSO was added to controls at respective concentrations. Incubation times depended on the specific assay and varied between few minutes and several days as specified in tables and figures.

Cytotoxicity assays

Cytotoxicity of the inhibitors was determined by the 3-[4,5-dimethylthiazol-2-yl]-2,5-diphenyl tetrazolium bromide (MTT) assay as described [41]. Cellular ATP content was determined using the CellTiter-Glo assay as described previously [47].

Enzymatic measurements and other analytical procedures

Preparation of cell lysates

Glycogen synthase activity was determined in cell lysates. Hepatocytes were washed with ice-cold saline before 200 μ l lysis buffer (50 mM Tris HCl, pH 7.4, 0.27 M sucrose, 1 mM Na₃VO₄, pH 10, 1 mM ethylenediaminetetraacetic acid (EDTA), 1 mM EGTA, 10 mM sodium- β -glycerophosphate, 50 mM NaF, 5 mM sodium pyrophosphate, 1% (x/v) Triton X-100 and 0.1% (v/v) 2-mercaptoethanol) were added. Cells were scraped off, homogenized by sonication (Sonopuls, Bandelin, Berlin, Germany), centrifuged at 15,000 \times g for 10 min., and supernatants stored at -20° C.

Glycogen synthase assay

The activity of glycogen synthase was determined according to Cross *et al.* [48]. Briefly, 45 μ l cell lysate were added to 90 μ l assay buffer (67 mM Tris HCl, pH 7.5, 89 mM uridine diphospho-D-glucose, 6.7 mM EDTA, 5 mM dithiothreitol, 13 mg/ml glycogen) containing 1 μ Ci uridine diphospho-[6-³H]-D-glucose in the presence or absence of 20 mM glucose-6-phosphate. After incubation at 37 $^{\circ}$ C for 30 min., the reaction mixture was spotted onto Whatman ECH 2R filter paper and 3-times washed in 66% ethanol for 20 min. Filters were finally washed in acetone, air dried, and used for scintillation counting. Glycogen synthase activity was expressed as the ratio of the activity in the absence and in the presence of glucose-6-phosphate.

Glutamine synthetase assay

Enzymatic activity of glutamine synthetase was determined with the glutamyltransferase method modified as described by Gebhardt and Williams [49]. In each assay 100 μ l cell homogenate in Hank's buffered salt solution

were used. Cellular protein concentration was measured according to Bradford [50] and the specific activity of glutamine synthetase was expressed in mU/mg protein.

Determination of glycogen synthesis

Enzymatic determination

Hepatocytes were cultured for 26 hrs and then incubated in the presence or absence of additional glucose (5 mM), insulin (10^{-6} M) and inhibitors of GSK-3 β for further 24 hrs. Glycogen content was determined enzymatically in cell homogenates according to Pfeleiderer [51].

Radioactive determination

Glycogen synthesis was measured as follows: cells were incubated with insulin or test compounds (in DMSO) for 60 min. Thereafter, 2 μ Ci [¹⁴C]glucose was added to the culture medium and incubation was continued for 120 min. Medium was aspirated and the cells were washed with phosphate-buffered saline (PBS) and extracted with 20% (w/v) KOH for 1 hr at 37 $^{\circ}$ C. Then, 90 μ l carrier glycogen (1 mg/ml) and 540 μ l ethanol were added and glycogen precipitated overnight at -20° C. Precipitates were recovered by centrifugation at 1000 \times g for 20 min., resuspended and transferred to scintillation vials for counting.

Phosphorylation of glycogen synthase

Phosphorylation of glycogen synthase by GSK-3 was detected by Western blotting using a phospho-glycogen synthase (Ser 641) antibody (Cell Signaling Technology, Inc., Danvers, MA, USA) according to the recommendations of the supplier and similarly as described for other proteins [52]. As control the glycogen synthase (15B1) Rabbit mAb (Cell Signaling Technology, Inc.) was used. The second antibody was anti-rabbit-FC AP-labelled (AP156A) (Chemicon Int., Inc., Millipore, Schwalbach, Germany) diluted 1:4500. Cellular extracts used are specified in the legends of the respective figures.

De novo fatty acid synthesis

Fatty acid synthesis from [¹⁴C]acetate was determined according to [53]. Briefly, hepatocyte cultures at day 2 (26 hrs) were washed with PBS and the medium was replaced by culture medium A containing 0.75 mg/ml bovine serum albumin (fatty acid free, Sigma-Adrich, Taufkirchen, Germany). Hepatocytes were pre-incubated with test compounds and inhibitors at 10 μ M for 90 min. and then labelled with [¹⁴C]acetate for 120 min. Thereafter, cultures were washed with PBS. The cells were scraped off into aqueous KOH (5% w/v) and saponified for 90 min. at 95 $^{\circ}$ C. Non-saponified lipids were extracted three times with petroleum ether and the residual aqueous phase was acidified with conc. HCl. Total fatty acids were repeatedly extracted with petroleum ether and the combined extracts were washed with 1% acetate before being dried in scintillation vials. After adding of 5 ml Ultima-Gold, radioactivity was counted in a liquid scintillation counter (Tri-carb 2500TR).

RNA isolation, cDNA synthesis and RT-PCR

Total cellular RNA from C17.2 cells was isolated using the NucleoSpin RNA II kit according to instructions of the manufacturer (Macherey-Nagel, Düren, Germany). Oligo dT-primed synthesis of cDNA was done with 1 µg total RNA and superscript II reverse transcriptase (Invitrogen GmbH, Karlsruhe, Germany). One-twentieth of each cDNA sample served as template in polymerase chain reactions with primers for murine Axin2 (forward: 5'-TCCCCACCTTGAATGAAGAA-3', reverse: 5'-TGGTGGCTGGT-GCAAAGA-3') and glyceraldehyde-3-phosphate dehydrogenase (GAPDH; forward: 5'-ACCACAGTCCATGCCATCACT-3', reverse: 5'-GTCCACCACCT-GTTGCTGTA-3'). Axin2 sequences were amplified using 32 cycles each consisting of 15 sec. at 96°C, 30 sec. at 56°C and 45 sec. at 72°C. GAPDH sequences were amplified using 20 cycles each consisting of 15 sec. at 96°C, 30 sec. at 56°C and 45 sec. at 72°C. One-tenth of each PCR reaction was loaded on non-denaturing 8% polyacrylamide gels with 0.5× Tris/borate/EDTA running buffer, and visualized by staining with ethidium bromide.

Expression and purification of glutathione S-transferase (GST) fusion proteins

Expression vectors for GST and GST fusion proteins with β-catenin residues 536–781, and the cytoplasmic tail of E-cadherin (GST-ECT) have been described [54, 55]. A construct for expressing GST-β-catenin 400–781 was obtained by inserting a *StuI/NotI* restriction fragment from pGEX4T1-β-catenin [54] into the *SmaI* and *NotI* sites of pGEX4T1 (Amersham Pharmacia, Freiburg, Germany). GST fusion proteins were expressed in *E. coli* BL21 and purified on glutathione sepharose as described [54] except for GST-β-catenin 400–781, which did not bind to glutathione sepharose and, therefore, was used as crude bacterial lysate.

Measurements of β-catenin activation

Changes in total amounts of β-catenin and in levels of hypophosphorylated β-catenin indicative of the activation of Wnt signalling in response to inhibition of GSK-3β or to the addition of Wnt-3α were followed by Western blotting. For this, protein extracts were made by lysing cells in ice-cold IPN150 buffer (50mM Tris/HCl H 7.6, 5 mM MgCl₂, 0.1% NP-40, 150 mM NaCl, 1mM DTT, 0.1 mM Na₃VO₄, 1 mM NaF, 1 mM PMSF and Complete protease inhibitor (Roche Applied Science, Mannheim, Germany) for 30 min. on ice with occasional mixing. After cell lysis, samples were centrifuged at 20,000 × *g* for 10 min. and the protein concentration of cleared supernatant was determined (DC protein assay, BioRad, Laboratories GmbH, München, Germany). Fractions of cellular lysates with 20 µg total protein were separated by SDS-PAGE on 10% gels. Prior to loading, each sample received a mixture with 2.5 ng of two GST fusion proteins carrying the amino acid residues 400–781, and 536–781 of β-catenin. These calibrator proteins served to monitor the efficacy of the Western blotting procedure and allowed normalization of the results upon quantification using the Lumilimager and the LumiAnalyst Software (Roche Applied Science). After transfer onto nitrocellulose membranes, Western blots were sequentially probed with anti-β-catenin primary antibodies (clone 14, BD Pharmingen; clone 8E7, Upstate Biotechnology), α-tubulin primary antibodies (clone DM 1A, Sigma-Aldrich, Taufkirchen, Germany), and the appropriate horseradish peroxidase-labelled secondary antibodies (Jackson ImmunoResearch, Europe Ltd., Suffolk, UK). Antibody/antigen complexes were visualized by

chemiluminescence (ECL system, Amersham Pharmacia). For affinity purification of the free cytoplasmic pool of β-catenin, 1 µg of GST or GST-ECT fusion proteins, 12.5 µl bed volume of glutathione sepharose beads, and cell lysate with a protein content of 500 µg were combined. The assay volume was adjusted to 500 µl with IPN150. Binding reactions were incubated at 4°C with constant agitation over night. Following extensive washing with IPN150, the material retained on the glutathione sepharose was eluted in SDS-PAGE loading buffer, separated by SDS-PAGE on 10% gels and analysed by Western blotting as above.

Alternatively, phosphorylated β-catenin was detected by the phospho-β-catenin (Ser33/37/Thr41) antibody (Cell Signaling Technology, Inc.) in Western Blots. The second antibody was anti-rabbit-FC AP-labelled (AP156A) (Chemicon Int., Inc.) diluted 1:4500.

Transfection experiments and reporter genes

For transfection HuH7 cells were cultivated at 0.25×10^6 cells per well in six-well plated in 1.5 ml of medium. Twenty-four hours after the start of the culture, transfection with the TCF reporter genes TOP-flash and FOP-flash (Upstate Biotechnology) was performed similar as described recently [56]. As transfection agent JetPEI (Qbiogene Inc., Irvine, CA, USA) was used and reporter activity was measured 24 hrs after transfection as described [57]. For reporter gene experiments with HEK293 cells, 1×10^5 cells were plated per well of 24-well plates. Cells were transfected with the TOP-flash reporter and the Renilla luciferase expression vector pRL-TK (Promega) for normalization purposes using the FuGENE6 reagent (Roche Applied Science, Mannheim, Germany).

Molecular docking procedures

The protein ligand docking studies were performed on the basis of the crystal structures of GSK-3β in complex with AR-A014418 (pdb entry 1q5k) [58]. The inhibitor and all solvent molecules were removed from the protein and polar hydrogen atoms were added using the Molecular Operating Environment software package (MOE 2005.06, Chemical Computing Group Inc., Montreal, Canada). After assigning Amber89 template charges, the protein was subjected to a stepwise energy minimization employing the Amber89 force field implemented in MOE 2005.06. First, only the positions of the side chains were optimized keeping the backbone atoms fixed at their crystallographic positions. Then, the backbone atoms were also allowed to move and the protein was minimized until convergence.

The ligand molecule was modelled using the molecular modelling program Spartan 5.0 (Wavefunction Inc., Irvine, CA, USA). The charges of the ligand atoms were derived from the electrostatic potential obtained on the basis of the semi-empirical quantum chemical method AM1 [59]. Non-polar hydrogens were merged into the adjacent carbon atoms employing the program AutoTors, which is part of the AutoDock 3.05 docking program package [60]. This program allows also the definition of the freely rotatable bonds of the ligand. The automated docking calculations were performed with the docking program AutoDock 3.05 [60] employing a two-step strategy: For the blind docking studies, the whole protein surface was searched for a preferred binding site within a grid box 15 Å larger than the extension of the protein in each direction. Subsequent dockings were performed within a user-specified three-dimensional box of $34 \times 34 \times 34$ Å centred on the co-crystallized inhibitor AR-A014418. Fifty independent docking runs for the ligand, employing the Lamarckian genetic algorithm implemented in AutoDock 3, were initiated with 100 randomly chosen

protein-ligand poses and iterated through up to 1.75 million energy evaluations. The resulting protein-ligand complexes were clustered with a tolerance of 1.0 Å. All other parameters were set to their default values as given in [60].

Results

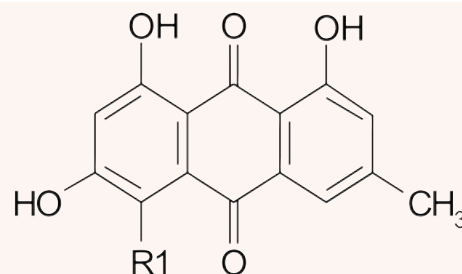
Protein kinase inhibition

Comparing emodin and its derivative 4-[N-(2-(aminoethyl)-amino)-emodin (L4) (Fig. 1) with respect to inhibition of protein kinases revealed that emodin – in close agreement with literature [35, 36] – inhibits CK-2 (not shown), while L4 preferentially inhibits GSK-3 β (Fig. 2). Respective IC₅₀-values derived from inhibition curves with GSK-3 β , CK-1 and CK-2 fitted by non-linear regression are shown for emodin and L4 in Table 1 and are compared with that of the established GSK-3 β inhibitor TDZD-8. Obviously, L4 is a strong inhibitor of GSK-3 β (more than 10-fold more active than TDZD-8). However, at least with respect to CK-1 and CK-2, L4 is slightly less discriminative than TDZD-8. In order to learn more about the specificity of L4, we tested the inhibitory potential of L4 and emodin at the fixed concentration of 10 μ M towards an extended panel of protein Ser/Thr kinases and protein tyrosine kinases frequently recognized to be affected by other inhibitors of GSK-3 β . As obvious from this comparison (Table 2), L4 does not strongly affect these kinases with the exception of AMPK and JNK-3 which are inhibited by 85% to 90%. Similar effects were found for SB216763. In contrast, emodin shows a completely different preference and affects particularly CDK-2/cyclin A, EGFR and PKC- α . At a concentration of 10 μ M, L4 was found to be almost as effective as SB216763 in inhibiting GSK-3 β (remaining activity 2% versus 1%). It also inhibits GSK-3 α (not shown).

Molecular docking studies

More insight into the molecular interactions of the emodin derivative L4 with GSK-3 β could be obtained from molecular docking studies. The blind docking strategy, which searches for possible binding sites on the complete protein surface area of GSK-3 β predicts the inhibitor L4 mostly bound in the ATP binding region in 50 independent docking experiments (Fig. 3A). This indicates that L4 preferentially interacts with the ATP-binding site.

A more detailed docking focussed on the ATP binding pocket of GSK-3 β . As shown in Fig. 3B, L4 is predicted to interact with the key residues Asp133 and Val135. These residues are reported to be essential for inhibitor binding [12, 58]. A closer look at the docked protein-inhibitor complex revealed that the backbone carboxyl group of Asp133 interacts with the 3-hydroxyl moiety of the emodin scaffold. The 1-hydroxyl group is involved in hydrogen bonds with the backbone of Val135. Additionally, the primary amino group of L4 interacts with the backbone carboxyl group of Val135.



Substance:

R1

Emodin

H

L4

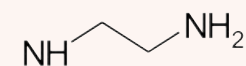


Fig. 1 Basal structure of emodin and 4-aminoethylamino-emodin (L4).

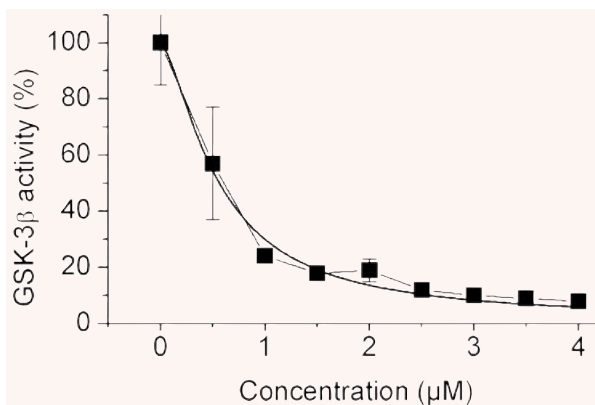


Fig. 2 Concentration-dependent inhibition of glycogen synthase kinase-3 β (GSK-3 β) by L4. Activity of GSK-3 β in response to different concentrations of L4, curve fitting and determination of IC₅₀-values were performed as described in 'Materials and methods'. Enzyme activity is expressed as percentage of the activity measured in the presence of DMSO. Data points (squares) represent means \pm S.D. of three independent measurements. The continuous thin line illustrates the result of curve fitting for determination of the IC₅₀-value.

Table 1 Comparison of IC₅₀ values for the inhibition of protein kinases GSK-3 β , CK-1 and CK-2 by emodin, 4-aminoethylamino-emodin (L4) and TDZD-8

Compound	IC ₅₀ -value (μ M)		
	GSK-3 β	CK-1	CK-2
emodin	16.5 \pm 0.6	14.1 \pm 0.3	0.3 \pm 0.01
L4	0.56 \pm 0.02	7.6 \pm 0.4	3.9 \pm 0.3
TDZD-8	7.1 \pm 0.3	>100*	>100*

*Estimated, because of limited solubility of TDZD-8.

Table 2 Comparison of the influence of emodin, 4-aminoethylamino-emodin (L4) and SB216763 on the activity of 12 protein kinases *in vitro*

Protein kinase	Remaining kinase activity (%)*		
	Emodin	L4	SB2167631
GSK-3 β	63 \pm 4 [†]	2.1 \pm 1	1.1 \pm 0.4
AMPK (r) [‡]	40 \pm 3	14 \pm 2	12 \pm 1
CDK-2/cyclin A (h)	27 \pm 0	40 \pm 1	8 \pm 3
CDK-3/cyclin E (h)	74 \pm 1	100 \pm 2	n.d. [§]
EGFR (h)	32 \pm 6	76 \pm 9	85 \pm 4
FGFR-3 (h)	56 \pm 8	35 \pm 9	n.d.
JNK-3 (h)	38 \pm 4	10 \pm 0	23 \pm 2
MAPK-1 (h)	58 \pm 1	46 \pm 3	n.d.
MAPKAP-K2 (h)	87 \pm 2	39 \pm 0	n.d.
MSK-1 (h)	79 \pm 9	61 \pm 2	16 \pm 5
PKC- α (h)	8 \pm 1	75 \pm 8	86 \pm 7
PKC- β ₂ (h)	95 \pm 1	104 \pm 1	n.d.

*Results shown are presented as the difference between the percentage of the activity in the presence and absence of each inhibitor.

[†]Values represent means \pm range of duplicate determinations.

[‡]Recombinant enzyme with rat (r) or human (h) sequence.

[§]n.d., not determined.

Cytotoxicity studies

Before physiological effects of emodin derivative L4 and other GSK-3 inhibitors were studied in cellular systems, cytotoxicity of these compounds was determined over a wide range of concentrations using the MTT assay. Figure 4A shows that L4 was without any influence on hepatocyte viability up to the highest concentration of 400 μ M (close to its solubility limit) within a 24-hr exposure period. SB216763 was slightly more cytotoxic leading to some

decline of viability of hepatocytes above 100 μ M. In contrast, TDZD-8 diminished viability above 10 μ M and led to complete death of hepatocytes at 100 μ M. This strong cytotoxicity of TDZD-8 is reminiscent to rapid induction of apoptosis in other cells by this compound [61].

Cellular ATP levels, which responded more sensitively, correlated well with cytotoxicity determined with MTT in the case of SB216763 and TDZD-8 (Fig. 4B). While ATP levels were least affected by SB216763 up to 400 μ M, they approached almost zero values after exposure to 100 μ M of TDZD-8. Interestingly, L4 considerably diminished ATP levels at higher concentrations. At 50 μ M, approximately 75% ATP of the controls still remained in the cells, whereas at 100 μ M the ATP levels already dropped down to 10% (Fig. 4B). At concentrations above 100 μ M L4 maintained low, but measurable levels of ATP in the range of 2 to 5 μ M. Most interestingly, however, ATP levels were almost completely reversed upon removal of L4 after 10 hrs, but not those in the case of TDZD-8 (not shown).

Influence of L4 on glycogen synthase activity, glycogen content and fatty acid synthesis in cultured hepatocytes

GSK-3 β is a constitutively active kinase which phosphorylates a large number of different protein substrates [10, 13]. The best example studied is glycogen synthase which is also one of the key targets with respect to type 2 diabetes. Therefore, we determined alterations in glycogen synthase activity in cell homogenates and in a cell-based assay in response to insulin, GSK-3 inhibitors, and combinations thereof. Cultured hepatocytes were exposed to these compounds for 120 min. As depicted in Fig. 5A, insulin stimulated glycogen synthase activity determined in cell homogenates more than 3.5-fold. The GSK-3 inhibitors LiCl, L4 and SB216763 also induced a significant activation of glycogen synthase by about 2.8-, 3.3- and 2.6-fold, respectively. When insulin was combined with either L4 or SB216763, stimulation was enhanced to 5.8- and 5.4-fold, respectively (Fig. 5A). Similar effects of insulin, of the inhibitors, and of their combinations were found, when glycogen synthesis was directly measured in hepatocytes by incorporation of [¹⁴C]glucose (Fig. S1). Using this assay, it could be demonstrated that stimulation of glycogen synthesis by increasing concentrations of L4 showed a dependence similar to that in response to SB216763 (Fig. 5B). Furthermore, the acute influence of L4 on glycogen synthesis was mirrored in the long run by a significant increase of hepatocellular glycogen content. Within 24 hrs of incubation in normal culture medium (containing 11 mM glucose), glycogen content in the presence of L4 and SB216763 increased by 36% and 28%, respectively, compared to controls (11 mM glucose) which were set 100% (Fig. 5C). Under these conditions 10⁻⁷ M insulin approximately doubled glycogen content. The relationship between insulin and the inhibitors considerably changed, if glucose concentration was increased to 16 mM. Now, insulin increased glycogen content only by about 70%

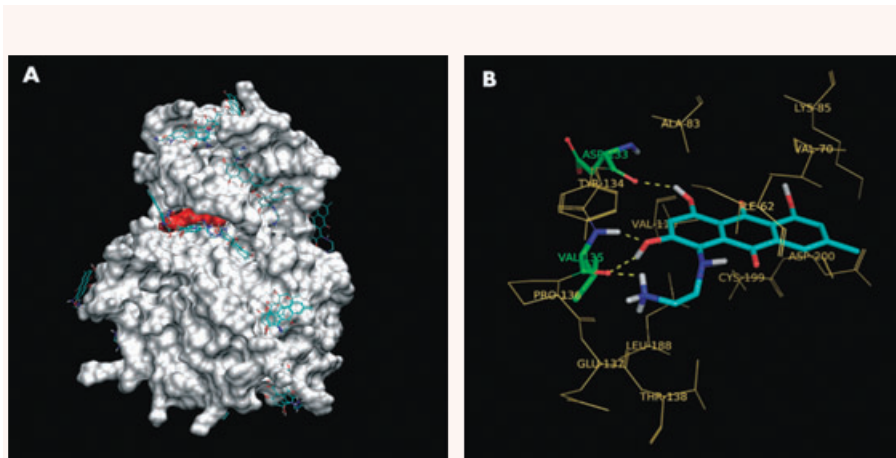


Fig. 3 Molecular docking of L4 to glycogen synthase kinase 3 β (GSK-3 β). **(A)** Overlay of 50 independent blind docking runs searching the complete protein surface for possible binding sites. The most preferred binding position is shown in red and is located in the ATP binding region. **(B)** Interaction of L4 with amino acid residues in the ATP-binding pocket of GSK-3 β obtained by detailed docking studies. Residues of the protein interacting with the inhibitor are represented as sticks in green. The inhibitor L4 is shown in cyan. Residues forming the ATP-binding pocket are shown as lines. Non-polar hydrogen atoms have been omitted for clarity.

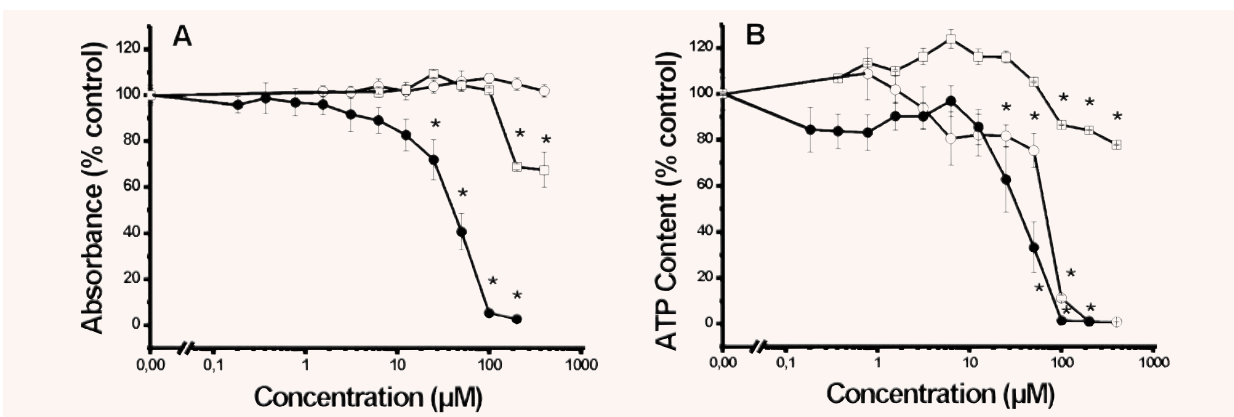


Fig. 4 Influence of emodin-derivative L4 and of two known inhibitors of GSK-3 β on **(A)** viability and **(B)** cellular ATP levels of cultured hepatocytes. **(A)** Cytotoxicity determined with the MTT assay. **(B)** ATP levels of hepatocytes expressed as percentage of DMSO control cultures. In both assays, cultured hepatocytes were exposed to L4 (open circles), TDZD-8 (closed circles) and SB216763 (open squares) for 24 hrs. Values represent means \pm S.D. of **(A)** three or **(B)** six independent measurements. *, significantly different from controls, $P < 0.01$.

compared to the new control value, while stimulation by L4 and by SB216763 reached about 90% and 63%, respectively (Fig. 5C). Similar results were found with mouse hepatocytes (Table S1). These findings demonstrate the insulin-sensitizing effect of L4 in cultured rodent hepatocytes and suggest an adequate response on glycogen synthesis particularly in the presence of elevated concentrations of glucose.

Furthermore, we determined the response of periportal and pericentral subpopulations of rat hepatocytes. Although the influence of insulin, GSK-3 inhibitors and of glucose concentration on glycogen content showed similar features as in total hepatocyte preparations, pericentral subpopulations apparently responded more strongly than periportal hepatocytes (Table S1). These results indicate the preferred response of pericentral hepatocyte subpopulations to L4.

A different set of experiments focused on acetate incorporation into newly synthesized fatty acids, because acetyl CoA carboxylase, one of the key enzymes of this pathway, is another important target of GSK-3 β [10]. As shown in Table 3, L4 was slightly less stimulatory than 10^{-7} M insulin, but still significantly enhanced acetate incorporation by about 30%. In the presence of both effectors incorporation was considerably reinforced. Similar, but less pronounced results were obtained with SB216763 at the same concentrations. When insulin concentration was raised to 2×10^{-6} M an increase of acetate incorporation by more than 110% was observed which could not be altered by further increasing insulin concentration. Under these conditions simultaneous presence of L4 did not alter acetate incorporation, too (Table 3). Using primary cultures of human hepatocytes similar results were found for 10 μ M of L4 or of AR

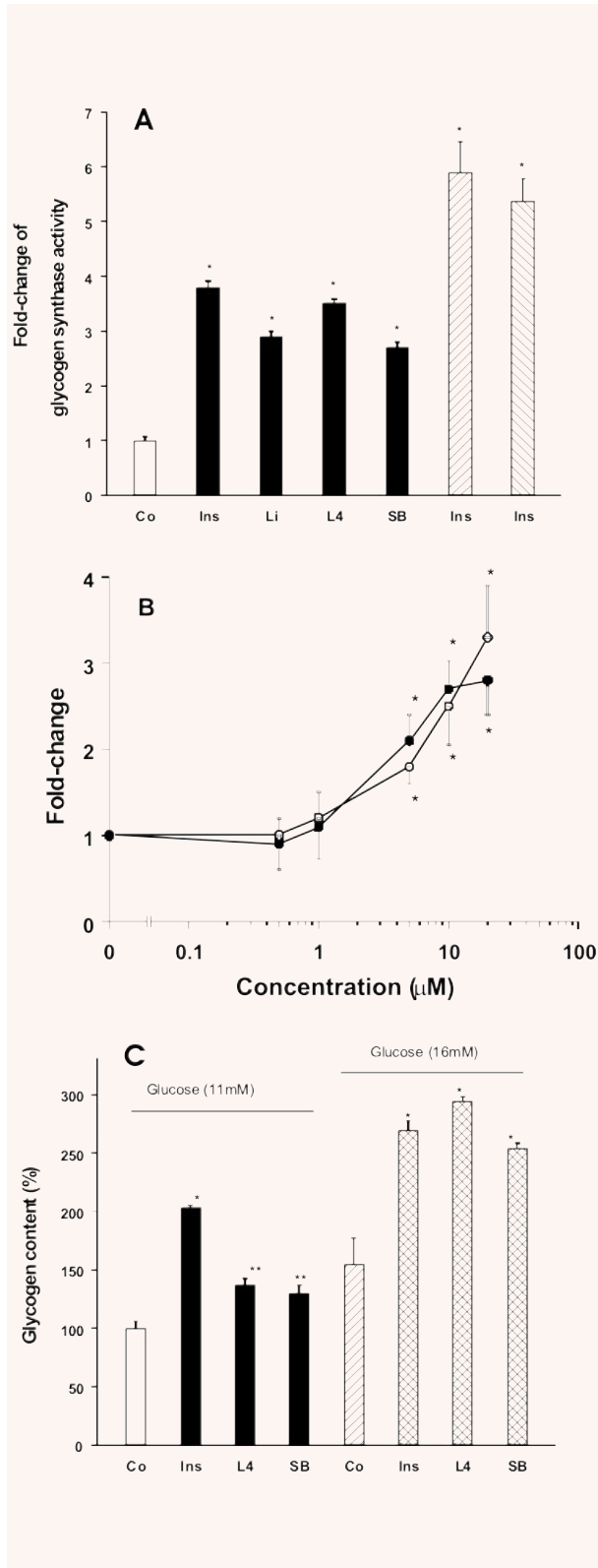


Table 3 Influence of GSK-3 β inhibitors on free fatty acid synthesis from radio-labelled [14 C]acetate in rat hepatocytes

Inhibitor	Acetate incorporation (%) [†]		
	Control	Insulin	
		(10 ⁻⁷ M)	(2 \times 10 ⁻⁶ M)
None	100 \pm 4 [‡]	134 \pm 6	217 \pm 12
L4	129 \pm 3*	167 \pm 7*	221 \pm 9
SB216763	122 \pm 4*	148 \pm 7*	n.d.

[†] Acetate incorporation was expressed as percent of controls in the absence of insulin and GSK-3, inhibitors.

[‡] Values represent means \pm S.D. of three determinations.

* Significantly different from respective controls: $P < 0.01$; n.d., not determined.



Fig. 5 Influence of insulin and different inhibitors of GSK-3 β on (A) glycogen synthase activity, (B) glycogen synthesis and (C) total glycogen in cultured hepatocytes. (A) Activation of glycogen synthase activity. Cultured hepatocytes were maintained in the presence of insulin (Ins, 10⁻⁷ M), the inhibitors lithium chloride (Li, 30 mM), L4 (10 μ M) and SB216763 (SB, 10 μ M) or in the presence of a combination of insulin with L4 (I + L4) and SB216763 (I + SB) for 90 min. Control cultures (Co) were exposed to the vehicle DMSO. Cells were lysed and the activity of glycogen synthase was measured as described in 'Materials and methods'. Results are expressed as fold-change of activities determined for control cells. Values represent means \pm S.D. of three independent determinations. *, significantly different from controls, $P < 0.001$; **, significantly different from controls, $P < 0.01$. (B) Concentration-dependence of the influence of L4 and SB216763 on glycogen synthesis. Cultured hepatocytes were incubated in the presence of inhibitors L4 (open circles) and SB216763 (closed circles) for 60 min. and exposed to [14 C]glucose for further 120 min. Cells were homogenized and glycogen synthesis was determined by scintillation counting as described in 'Materials and methods'. Results are expressed as fold-change of the synthetic capacity determined for control cells. Values represent means \pm S.D. of three independent determinations (for clarity, S.D. is shown one-sided with variable orientation). (C) Influence of insulin and different inhibitors of GSK-3 β on total glycogen in cultured hepatocytes. Hepatocytes were cultured in the presence of insulin (Ins, 10⁻⁷ M) or the inhibitors L4 (10 μ M) and SB216763 (SB, 10 μ M) for 24 hrs. Incubation was performed in normal culture medium (11 mM glucose) or after addition of 5mM glucose (16 mM glucose). Thereafter, cells were homogenized and glycogen content was determined enzymatically as described in 'Materials and methods'. Results are expressed as percentage of the content of control cultures. Values represent means \pm S.D. of three independent determinations. *, significantly different from controls, $P < 0.01$; **, significantly different from controls, $P < 0.05$.

A014418, one of the most specific inhibitors of GSK-3 [22] (data not shown).

Stabilization of β -catenin by GSK-3 β inhibitors

GSK-3 β plays a major role in Wnt signal transduction by mediating degradation of β -catenin [33]. Abrogating GSK-3 β -dependent phosphorylation of β -catenin by Wnt growth factors or chemical inhibitors of GSK-3 β , leads to the accumulation of hypophosphorylated, uncomplexed β -catenin in the cytosol and nucleus where it induces target gene transcription [33]. To analyse whether inhibition of GSK-3 β by L4 had any effect on Wnt/ β -catenin pathway activity we monitored overall levels of β -catenin and its signalling-competent hypophosphorylated isoforms in HEK293 human embryonic kidney cells. Upon treatment with increasing concentrations of L4, whole cell lysates were prepared 3 hrs after stimulation and used for Western blotting. For comparison, dose-dependent effects of two other GSK-3 β inhibitors, LiCl and SB216763 were studied [33]. As shown in Fig. 6A, LiCl and SB216763 produced pronounced increases of the levels of hypophosphorylated β -catenin as revealed by the anti-active- β -catenin (anti-ABC) antibody [62, 63]. In parallel, a concomitant surge in total amounts of β -catenin was detected with an antibody recognizing the C-terminus of β -catenin (Fig. 6B). However, the effect on total cellular β -catenin was less pronounced. Presumably, a pre-existing population of β -catenin involved in cell-cell adhesion largely masks the free pool of β -catenin which gradually builds up in the presence of the GSK-3 β inhibitors. Compared to LiCl and SB216763, L4 had only minor effects on β -catenin amounts and phosphorylation state. The dose-dependent response showed its maximum effect with 80 μ M L4, whereas LiCl and SB216763 produced much stronger effects with optimal concentrations around 40 mM (LiCl) and 20 μ M (SB216763), respectively. When used at higher concentrations, all three substances exhibited toxic effects and reduced cell viability. In the case of LiCl, this is clearly visible by the decrease in total cellular protein content as indicated by the diminished signals of β -catenin and the α -tubulin loading control (Fig. 6A–C, lanes 11 and 12).

To determine whether reduced efficacy of L4 at activating β -catenin was specific for HEK293 cells, we additionally examined the effects of L4, SB216763 and Wnt-3 α -conditioned media in the neural cell line C17.2 which is known to respond well to activation of Wnt/ β -catenin signalling [64]. Western blot analyses of whole cell lysates showed no change in overall levels of β -catenin in response to inhibition of GSK-3 β (Fig. 6E). Again, this is likely due to high amounts of β -catenin present in cell adhesion complexes which prevent detection of the free pool of β -catenin induced by the GSK-3 β inhibitors. Therefore, this signalling-competent pool of β -catenin was specifically measured by affinity precipitation (GST-ECT fishing) using a GST fusion protein containing the cytoplasmic tail of E-cadherin, a high affinity binding partner of β -catenin [65]. Treatment with SB216763 or Wnt-3 α led to a strong increase in the amount of β -catenin which could be recovered

by GST-ECT (Fig. 6D, compare lanes 2, 4, 8, 12). As in HEK293 cells, however, L4 produced a relatively minor effect (Fig. 6D, compare lanes 2, 4, 10).

In many cases, the ultimate cellular response towards a Wnt stimulus is a change in gene expression patterns [33]. To further examine potential effects of L4 on the activity of the Wnt/ β -catenin pathway we therefore asked whether L4 could induce transcription of a cognate β -catenin/TCF target gene. For this purpose, we stimulated the C17.2 with various concentrations of L4 for 6 hrs. Parallel cultures of C17.2 cells were treated with SB216763 or Wnt-3 α . RNA from stimulated and control cells was isolated, reverse transcribed and used for semi-quantitative PCRs with primers specific for Axin2, a gene which is highly inducible by Wnt-3 α or SB216763 in a wide range of cells [66–68]. As expected, both SB216763 and Wnt-3 α enhanced Axin2 expression (Fig. 7, lanes 3, 4 and 8, 9). In contrast, L4 failed to stimulate Axin2 transcription at all concentrations tested (Fig. 7, lanes 5–7). Thus, the lack of Axin2 induction correlates with the lesser capacity of L4 to induce a free pool of β -catenin. In summary, L4 is able to evoke a limited cytosolic response of the Wnt/ β -catenin pathway with some accumulation of hypophosphorylated β -catenin, but the degree of activation appears to be too low to elicit a nuclear response.

Differential induction of TCF-responsive targets by GSK-3 β inhibitors and L4

In order to obtain information on whether the lack of effect of L4 on expression of Axin2 is solely due to the low degree of β -catenin activation or may depend partly or fully on other features of L4, the response of two other TCF-responsive targets was investigated. First, we used a transient transfection assay with the TOPflash reporter in HuH7 cells. The non-responsive reporter FOPflash was used as control. As depicted in Fig. 8A, SB216763 considerably enhanced the ratio of TOPflash/FOPflash within 24 hrs after transfection. In contrast, L4 significantly reduced this ratio below that of controls. Most interestingly, however, when HuH7 cells were exposed to both SB216763 and L4, the stimulation obtained by SB216763 was blocked to a large extent (Fig. 8A).

Second, a similar type of experiment was performed in HEK293 cells transfected with the TOPflash reporter. In parallel to determination of TOPflash activity in the presence of control (DMSO), SB216763 (10 μ M), L4 (10 μ M) and the combination of both inhibitors the relative amount of β -catenin was determined by Western blotting (Fig. S2). While L4 had no influence on the relative amount of β -catenin and on TOPflash activity, it reduced the induction of both parameters by SB216763.

Third, we investigated the influence of these inhibitors on the expression of glutamine synthetase, which has recently been shown to be up-regulated by activating mutations of β -catenin [27, 69] or by lithium chloride [27] in hepatoma cells and foetal mouse hepatocytes [70]. As depicted in Fig. 8B, glutamine synthetase specific activity responds well to LiCl (up to 40 mM) in

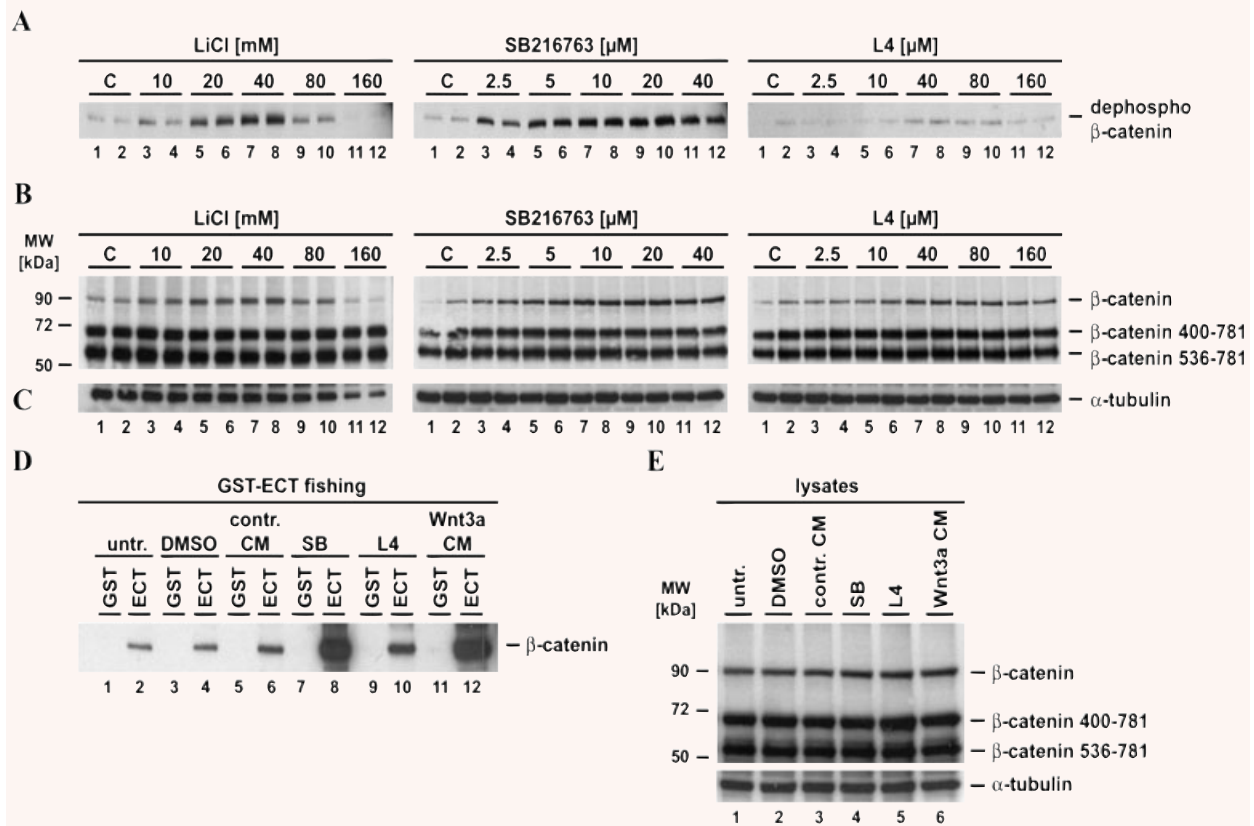


Fig. 6 Influence of different GSK-3 β inhibitors on total amount and activation of β -catenin. **(A)** Dose-dependent accumulation of activated and **(B)** total β -catenin in HEK293. Twenty-four hours before stimulation 0.5×10^6 HEK293 cells per well were seeded into six-well plates. To inhibit GSK-3 β , cells were treated with different concentrations of LiCl (10, 20, 40, 80 and 160 mM; lanes 3–12), SB216763 (2.5, 5, 10, 20 and 40 μ M; lanes 3–12) and L4 (2.5, 10, 40, 80 and 160 μ M; lanes 3–12). Controls were either untreated (LiCl; lanes 1, 2) or received DMSO at a final concentration of 0.8% (SB216763 and L4; lanes 1, 2). Cells were harvested 3 hrs after adding GSK-3 β inhibitors and cell lysates were prepared. After determination of protein concentrations and the addition of GST- β -catenin calibrator proteins, duplicate samples of each cell lysate were separated by SDS-PAGE, and subsequently transferred onto nitrocellulose. Western blots were sequentially probed with antibodies recognizing **(A)** active β -catenin (anti-ABC), **(B)** total cellular β -catenin and **(C)** α -tubulin. **(D)** Affinity precipitation to measure a signalling-competent pool of β -catenin induced by Wnt-3a or GSK-3 β inhibitors. Twenty-four hours before stimulation 5×10^6 murine C17.2 cells were seeded into 100 mm plates. To induce a free pool of β -catenin cells were treated with SB216763 (20 μ M), L4 (40 μ M) or Wnt-3a-conditioned media (Wnt-3a CM). Controls were either untreated, received DMSO at a final concentration of 0.4% or were incubated with mock conditioned media (cont. CM). Cells were harvested 3 hrs after adding GSK-3 β inhibitors or Wnt-3a CM and cell lysates were prepared. To recover the pool of free cytosolic β -catenin, samples of each cell lysate were supplemented with glutathione sepharose beads and either GST or the GST-ECT fusion protein as indicated. After the binding reaction and extensive washing, proteins bound to the glutathione sepharose matrix were eluted with SDS-PAGE loading buffer, separated by SDS-PAGE and analysed by Western blotting with an antibody recognizing β -catenin. Lanes 1, 2: untreated control cells; lanes 3, 4: DMSO-treated cells; lanes 5, 6: cells treated with mock-conditioned media; lanes 7, 8: SB216763-treated cells; lanes 9, 10: L4-treated cells; lanes 11, 12: cells treated with Wnt-3a-conditioned media. **(E)** In parallel, a sample of each lysate used for GST-ECT fishing was combined with a mixture with 2.5 ng of GST-fusion proteins carrying amino acid residues 400–781 and 536–781 of β -catenin and total levels of β -catenin were analysed by Western blotting with anti- β -catenin and anti- α -tubulin antibodies. MW: molecular weight marker.

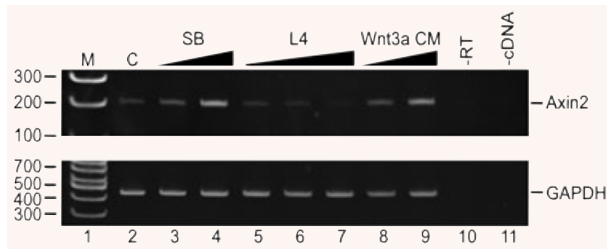


Fig. 7 Induction of Axin2 transcription by Wnt-3a or GSK-3 β inhibitors. Twenty-four hours before induction 5×10^5 C17.2 cells per well were seeded into six-well plates. To induce Axin2 transcription, SB216763 (final concentrations 5 μ M and 20 μ M; lanes 3, 4), L4 (final concentrations 10 μ M, 40 μ M or 160 μ M; lanes 5–7) or Wnt-3a-conditioned media (diluted 1:1 with growth media or undiluted; lanes 8, 9) were added to the cells. Control cells (C; lane 2) received DMSO (final concentration 0.4%). Cells were harvested and RNA was prepared 6 hrs after induction. Transcript levels of Axin2 and the GAPDH control were determined by semi-quantitative RT-PCR. Control reactions were carried out with a mock cDNA sample prepared in the absence of reverse transcriptase (-RT, lane 10) or without cDNA template (-cDNA, lane 11). PCR products were resolved by PAGE and visualized by staining with ethidium bromide. M: molecular weight marker.

HepG2 cells. Likewise, SB216763 provoked a dose-dependent increase in glutamine synthetase activity up to 40 μ M, while L4 did not change enzyme activity in the HepG2 cells even at concentrations of 40 μ M (Fig. 8C). If, however, SB216763 and L4 were combined, the SB216763-induced increase in enzyme activity was prevented by L4 in a concentration-dependent manner (Fig. 8D). A similar effect was observed when cells were simultaneously exposed to LiCl and L4. These results suggest that L4 exerts a general inhibition of β -catenin-dependent gene expression.

In order to learn more about the ability of L4 to counteract β -catenin-dependent gene expression and to reveal its relevance for the liver, another set of experiments was performed in primary mouse hepatocytes focussing on the three variables of interest, namely phosphorylation of glycogen synthase, phosphorylation of β -catenin and the pool of activated/free β -catenin. This was done side-by-side in the same extracts of hepatocytes exposed to either one of the stimuli Wnt-3a, SB216763 and L4 or some of their combinations for 3 hrs. As shown in Fig. 9A the fraction of phosphorylated glycogen synthase was differentially reduced by Wnt-3a and all GSK-3 inhibitors. In the simultaneous presence of L4 and Wnt-3a or SB216763 this reduction was reinforced. These effects seemed to be due not only to a decrease in phospho-glycogen synthase, but also to a slight increase in total glycogen synthase during the incubation period in the presence of GSK-3 inhibitors. Likewise, the amount of phospho- β -catenin was reduced in the presence of GSK-3 inhibiting agents and particularly of their combinations (Fig. 9A). Interestingly, however, the pool of β -catenin available for ECT-fishing (*i.e.* activated/free β -catenin) was increased only by Wnt-3a and SB216763, but not

by L4 (Fig. 9B) in agreement with the results shown in Fig. S2. Moreover, L4 was able to significantly decrease the effects of these two agents when present simultaneously (Fig. 9B). These results corroborate the results obtained with the reporter gene assays and suggest that some step between dephosphorylation of β -catenin and the occurrence of free β -catenin in a pool detectable by ECL fishing might be affected by L4.

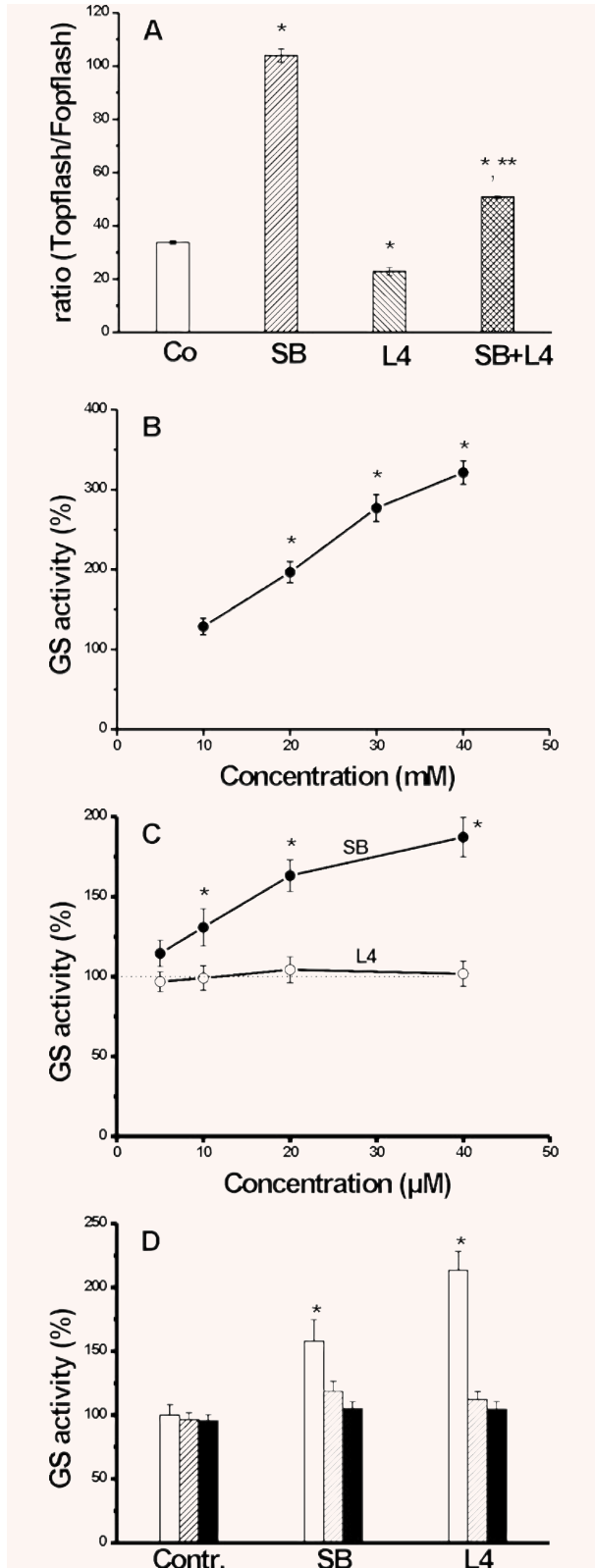
Discussion

According to a recent general survey on the specificity of GSK-3 β inhibitors [22] as well as to results from various original publications [71–74] exclusive specificity of synthetic inhibitors for this particular kinase is rare despite their considerable structural diversity. Rather, each inhibitor even the most specific ones, namely CT 99021 and AR A014418 [22, 25, 58], acts on at least one or two additional kinases of various kinds even though respective IC₅₀ values may indeed be somewhat higher than for GSK-3 β . In physiological terms, this means that each inhibitor may exert different effects within cells and tissues, although some central activities like stimulation of glycogen synthase may be common to almost all of them. The novel GSK-3 β inhibitor described herein, L4, fully fits into this scheme but shows interesting properties not reported before.

First, L4 seems to belong to the large group of ATP-competitive inhibitors. This is suggested by molecular docking studies demonstrating that L4 binds to the ATP binding region and closely interacts with key residues Asp133 and Val135 that seem to be essential for the binding of many other GSK-3 β inhibitors [12, 58, 72, 74–78]. Despite this similarity, however, L4 does inhibit neither CDKs nor PKC which are secondary targets of several ATP-competitive inhibitors [71, 74]. In contrast, L4 seems to affect to some extent two other kinases, namely JNK-3 and AMPK, which have rarely been described as secondary targets of GSK-3 β inhibitors.

Second, L4 shows a low cytotoxicity compared with many GSK-3 β inhibitors particularly with TDZD-8. Because of the complex role of GSK-3 β in regulating apoptosis [79] especially in hepatocytes [80], the outcome of inhibition of GSK-3 β may depend on secondary effects of the inhibitors used. In this respect, it is remarkable that TDZD-8 leads to apoptosis and hepatocytes death most probably because of irreversible loss of ATP levels above 20 μ M, while the drop in ATP levels in response to L4 is reversible and does not influence viability of the cells. This feature of L4 is reminiscent of the effects of fructose at concentrations in the upper millimolar range which lead to considerable stabilization of long-term survival of hepatocytes in culture [81], despite a rapid transient loss of ATP.

Third, our results demonstrate that L4 is a strong and long-lasting insulin-sensitizer with respect to hepatic glycogen and fatty acid metabolism. While stimulation of glycogen synthase activity in response to GSK-3 β inhibition has been reported for many different classes of inhibitors [11–13, 24], data on the influence on



fatty acid synthesis are essentially lacking. Here, we show that L4 in the hepatocellular context stimulates fatty acid synthesis from acetate similar to insulin at intermediate concentrations. In both cases, L4 acts in concert with suboptimal levels of insulin, while no such synergy was observed at high, optimal concentrations of insulin. In addition, we found that phosphorylation of glycogen synthase at Ser641 was reduced by L4. These findings strongly favour the assumption that the effect of L4 is mediated by inhibition of GSK-3 β , although it cannot be excluded that some inhibition of GSK-3 α is involved. Likewise, partial inhibition of AMPK may participate in stimulating fatty acid synthesis due to phosphorylation of acetyl-CoA carboxylase by AMPK [82].

Finally, compelling evidence is provided for prevention of TCF/LEF-dependent gene expression by L4 in response to activation of β -catenin. This feature of L4 which contrasts to the activation of β -catenin signalling by most GSK-3 β inhibitors [11, 23–25, 80] may help to elucidate the still open question why insulin, in the adult organism, can act through inhibition of GSK-3 β while circumventing activation of β -catenin. Obviously, zonation of liver parenchyma cannot play a role, because we observed a stronger influence of L4 on pericentral glycogen deposition, *i.e.* in the same zone where Wnt/ β -catenin signalling is most active in the liver [27]. Furthermore, L4 not only failed to activate β -catenin as strong as other GSK-3 β inhibitors, but rather it counteracted the activation of TCF/LEF target gene expression by other GSK-3 β inhibitors. This dual influence of L4 is illustrated in Fig. 10. We provide evidence that L4 acts through inhibition of a hitherto unknown event downstream to activation of β -catenin by dephosphorylation which precedes the occurrence of β -catenin in a cellular pool accessible to ECL fishing (Fig. 10). Importantly, this pool seems essential for switching on target gene expression as demonstrated by the response of three different reporter or target

Fig. 8 Influence of GSK-3 β inhibitors on (A) expression of the TOPflash reporter and (B–D) induction of glutamine synthetase. (A) Transient transfection experiment with HuH7 cells. HuH7 cells transfected with TOPflash and FOPflash reporters as described in ‘Materials and methods’ were cultured without inhibitor (Co), with SB216763 (10 μ M, SB), L4 (10 μ M, L4) or in the presence of both inhibitors (SB + L4) for 24 hrs. Values represent means + S.D. of six independent determinations and are expressed as percentage of control cultures. *, significantly different from control, $P < 0.01$; **, significantly different from SB or L4, $P < 0.01$. (B, C) HepG2 cells were cultured in the presence of the GSK-3 β inhibitors (B) LiCl (closed circles) and (C) SB216763 (closed circles) or L4 (open circles) for 48 hrs. Thereafter, cell homogenates were prepared and glutamine synthetase specific activity was determined as described in ‘Experimental procedures’. The dotted line in (C) indicates control level (=100%). (D) Simultaneous incubations of SB216763 (20 μ M) or LiCl (30 mM) in the presence of different concentrations of L4 (0 μ M, open bars; 5 μ M, hatched bars; 10 μ M, black bars) for 48 hrs. Thereafter, activity of glutamine synthetase was determined. (B–D) Values represent means + S.D. of three independent determinations and are expressed as percentage of control cultures in the absence of inhibitor. *, significantly different from controls, $P < 0.01$.

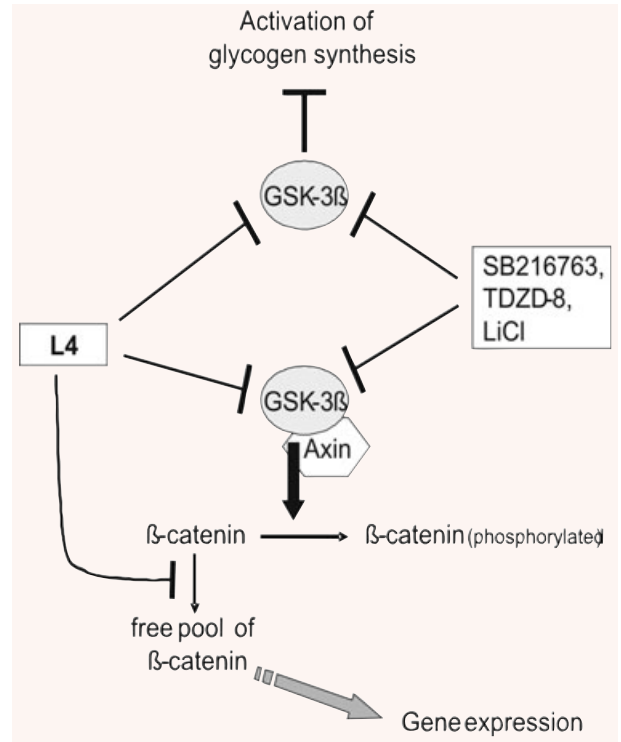
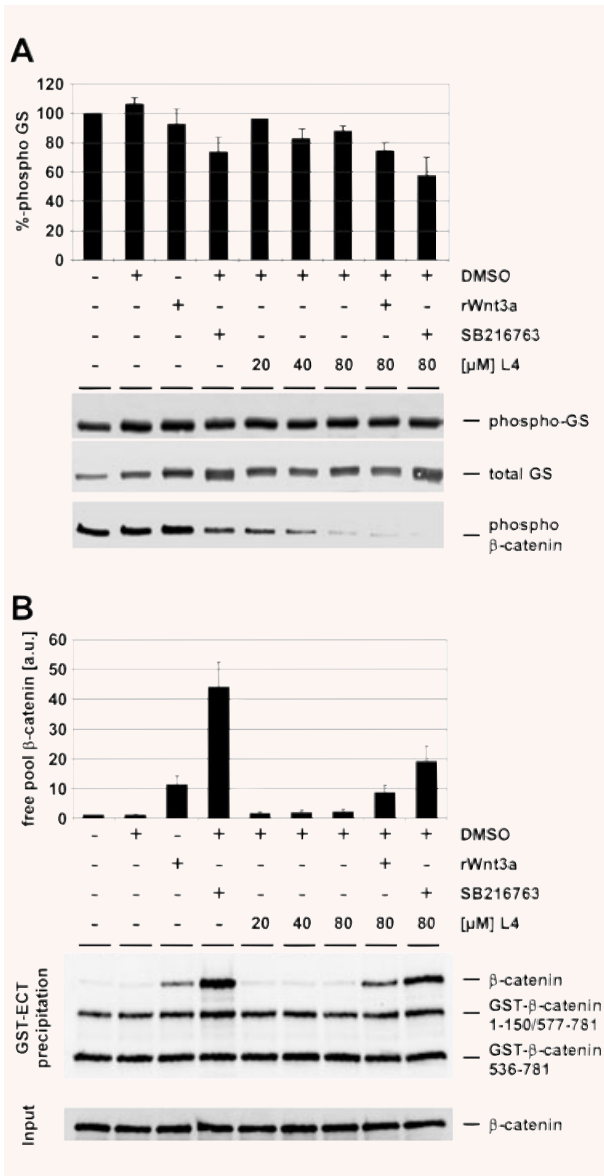


Fig. 10 Scheme illustrating the differential influence of the novel GSK-3β inhibitor L4 and of established inhibitors, SB216763, TDZD-8 and LiCl on metabolic events and β-catenin-dependent gene expression. Established inhibitors (SB216763, TDZD-8 and LiCl) inhibit GSK-3β irrespective of whether it is bound to Axin or not resulting in activation of metabolic events (e.g. glycogen synthesis) as well as β-catenin-dependent gene expression. The novel inhibitor L4 has a similar influence on GSK-3β, but additionally inhibits an event downstream to dephosphorylation of β-catenin. Thus, L4 favours activation of metabolic events, while avoiding β-catenin-dependent gene expression.

Fig. 9 Influence of GSK-3β inhibiting agents Wnt-3a, SB216763, L4 and combinations thereof on (A) phosphorylation of glycogen synthase and β-catenin and (B) a signalling-competent pool of β-catenin in primary mouse hepatocytes. Twenty-four hours before stimulation 2×10^6 primary murine hepatocytes were seeded into 60 mm plates. To induce phosphorylation events at glycogen synthase and β-catenin or a free pool of β-catenin cells were treated with 200 ng/ml recombinant Wnt-3a (rWnt-3a), 80 μM SB216763, increasing concentrations of L4, or combinations of these reagents as indicated. Control cells were left either untreated or received DMSO at a final concentration of 0.4%. Cells were harvested 3 hrs after adding Wnt-3a or the GSK-3 inhibitors, and cell lysates were prepared as in Fig. 6D. Part of this lysate was used (A) for Western Blots using phospho-glycogen synthase (Ser641) antibody, glycogen synthase (15B1) Rabbit mAb, and phospho-β-catenin (Ser33/37/Thr41) antibody or (B) for GST-ECT affinity precipitations as described in (Fig. 6D) using GST-β-catenin fusion proteins as normalizers as indicated. Western blotting signals were quantified and processed as described in 'Materials and methods' and in [80]. The results shown in (A) represent average values of phospho-glycogen synthase normalized to total glycogen synthase and those shown in (B) represent average values of normalized β-catenin amounts derived from the same three independent experiments. The corresponding standard errors are given. The results are expressed as (A) percentage of control cells (100%) or as (B) fold changes of β-catenin amounts relative to untreated control cells (=1).

genes. Potentially, this mechanism could provide an alternative explanation of how insulin discriminates between activation of glycogen synthesis and activation of β -catenin signalling in the liver. So far, two other explanations have been advanced for this differential influence of insulin, the sequestration of GSK-3 β by FRAT-1 [31] and the differential accessibility of Axin-bound GSK-3 β to insulin-induced phosphorylation at serine 9 [37]. None of these explanations has yet been substantiated at least for the liver. Thus, further investigation of the action of L4 may possibly provide also a clue for understanding the differential action of insulin. Regardless of whether this expectation will be met, L4 has proven to show efficient insulin-sensitizing activity with respect to metabolic regulation, while simultaneously avoiding or even reducing the potential risk of β -catenin activation. Therefore, it may add a new class of compounds to the list of potentially useful drugs [83] for future treatment of diseases like diabetes type 2, AD and other neurological disorders.

Acknowledgements

The excellent technical assistance of Mrs. K. Bruser, Mrs. K. Heise, Mrs. D. Mahn and Mr. F. Struck is gratefully acknowledged. Furthermore, we thank an unknown reviewer for his constructive comments. This study was supported in part by grants from the Deutsche Forschungsgemeinschaft (projects Ge 465/7-2 and Ge 465/8-1), SFB 610 'Variation in protein Conformation: Cell biological and Pathological relevance' (projects B3 and Z3, R.G. and H.-J.H.) and BMBF research grant 0313074D HepatoSys, project B3 to A.H.

Supporting Information

Additional Supporting Information may be found in the online version of this article:

Fig. S1 Influence of insulin and different inhibitors of GSK-3 β on glycogen synthesis in cultured hepatocytes. Cultured hepatocytes were maintained in the presence of insulin (Ins, 10^{-7} M), the inhibitors lithium chloride (Li, 30 mM), L4 (10 μ M) and SB216763

(SB, 10 μ M) or in the presence of a combination of insulin with L4 (I + L4) and SB216763 (I + SB). Control cultures (Co) were exposed to the vehicle DMSO. After 60 min., [14 C]glucose was added and incubation was continued for 120 min. Thereafter, cells were homogenized and glycogen synthesis was determined by scintillation counting as described in 'Materials and methods'. Results are expressed as fold-change of the synthetic capacity determined for control cells. Values represent means + S.D. of three independent determinations. *, significantly different from controls, $P < 0.001$; **, significantly different from controls, $P < 0.01$.

Fig. S2 Influence of GSK-3 β inhibitors on (A) expression of the TOP-flash reporter and (B, C) β -catenin protein levels in HEK293 cells. (A) HEK293 cells were transiently transfected with the TOP-flash reporter plasmid as described in 'Materials and methods'. Transfected cells were cultured without inhibitor (DMSO), with SB216763 (10 μ M, SB), L4 (10 μ M, L4) or in the presence of both inhibitors (SB + L4) for 24 hrs. The results shown represent average activities derived from three independent experiments and the corresponding standard deviations. They are expressed as relative activities (rel. act.) compared to cells kept in the presence of the solvent control DMSO only (rel. act. = 1). (B, C) The presence of L4 reduces β -catenin protein amounts induced by SB216763. Whole cell lysates prepared from transfected cells used for luciferase measurements in (A) were separated by SDS-PAGE and analysed by Western blotting with antibodies against β -catenin, and α -tubulin to check for equal loading. β -Catenin and α -tubulin signals were recorded with a Lumilimager and processed using α -tubulin for normalization. Normalized levels of β -catenin are displayed in (B). The results shown represent average values derived from three independent experiments and the corresponding standard errors. β -Catenin levels are expressed as relative amounts compared to cells treated with DMSO only (rel. amount = 1).

Table S1. Glycogen content in rat and mouse hepatocyte populations

Please note: Wiley-Blackwell are not responsible for the content or functionality of any supporting information supplied by the authors. Any queries (other than missing material) should be directed to the corresponding author for the article.

References

1. Hanada M, Feng J, Hemmings BA. Structure, regulation and function of PKB/AKT – a major therapeutic target. *Biochem. Biophys. Acta.* 2004; 1697: 3–16.
2. Dong LQ, Feng L. PDK2: the missing piece in the receptor tyrosine kinase signaling pathway puzzle. *Am J Physiol Endocrinol Metab.* 2005; 289: E187–96.
3. McManus EJ, Sakamoto K, Armit LJ, *et al.* Role that phosphorylation of GSK-3 plays in insulin and Wnt signalling defined by knockin analysis. *EMBO J.* 2005; 24: 1571–83.
4. Parker PJ, Caudwell FB, Cohen P. Glycogen synthase from rabbit skeletal muscle; effect of insulin on the state of phosphorylation of the seven phosphoserine residues *in vivo*. *Eur J Biochem.* 1983; 130: 227–34.
5. Furnsinn C, Noe C, Herdlicka R, *et al.* More marked stimulation by lithium than insulin of the glycogenic pathway in rat skeletal muscle. *Am J Physiol.* 1997; 273: E514–20.
6. Seo YH, Jung HJ, Shin HT, *et al.* Enhanced glycogenesis is involved in

- cellular senescence *via* GSK3/GS modulation. *Aging Cell*. 2008; 7: 894–907.
7. **Lochhead PA, Coghlan M, Rice SQ, et al.** Inhibition of GSK-3 selectively reduces glucose-6-phosphatase and phosphoenolpyruvate carboxykinase gene expression. *Diabetes*. 2001; 50: 937–46.
 8. **Kim KH, Song MJ, Yoo EJ, et al.** Regulatory role of glycogen synthase kinase 3 for transcriptional activity of ADD1/SREBP1c. *J Biol Chem*. 2004; 279: 51999–2006.
 9. **Bullock WH, Magnuson SR, Choi S, et al.** Prospects for kinase activity modulators in the treatment of diabetes and diabetic complications. *J Curr Top Med Chem*. 2002; 2: 915–38.
 10. **Doble BW, Woodgett JR.** GSK-3: tricks of the trade for a multi-tasking kinase. *J Cell Sci*. 2003; 116: 1175–86.
 11. **Cohen P, Goedert M.** GSK3 inhibitors: development and therapeutic potential. *Nature Rev Drug Disc*. 2004; 3: 479–87.
 12. **Meijer L, Flajole M, Greengard P.** Pharmacological inhibitors of glycogen synthase kinase 3. *Trends Pharmacol Sci*. 2004; 25: 471–80.
 13. **Forde JE, Dale TC.** Glycogen synthase kinase 3: a key regulator of cellular fate. *Cell Mol Life Sci*. 2007; 64: 1930–44.
 14. **Bhat RV, Haerberlein SLB, Avila J.** Glycogen synthase kinase 3: a drug target for CNS therapies. *J Neurosci*. 2004; 89: 1313–7.
 15. **Selenica ML, Jensen HS, Larsen AK, et al.** Efficacy of small-molecule glycogen synthase kinase-3 inhibitors in the postnatal rat model of tau hyperphosphorylation. *Brit J Pharmacol*. 2007; 152: 959–79.
 16. **Phiel CJ, Wilson CA, Lee VM, et al.** GSK-3 α regulates production of Alzheimer's disease amyloid- β peptides. *Nature*. 2003; 423: 435–9.
 17. **De Strooper B, Woodgett J.** Alzheimer's disease: mental plaque removal. *Nature*. 2003; 423: 392–3.
 18. **Muyllaert D, Kremer A, Jaworski T, et al.** Glycogen synthase kinase-3 β , or a link between amyloid and tau pathology? *Genes Brain Behav*. 2008; 7: 57–66.
 19. **Frame S, Zheleva D.** Targeting glycogen synthase kinase-3 in insulin signalling. *Expert Opin Ther Targets*. 2006; 10: 429–44.
 20. **Gould TD.** Targeting glycogen synthase kinase-3 as an approach to develop novel mood-stabilising medications. *Expert Opin Ther Targets*. 2006; 10: 377–92.
 21. **Murray JT, Cambell DG, Morrice N, et al.** Exploitation of KESTREL to identify NDRG family members as physiological substrates for SGK1 and GSK3. *Biochem J*. 2004; 384: 477–88.
 22. **Bain J, Plater L, Elliott M, et al.** The selectivity of protein kinase inhibitors: a further update. *Biochem J*. 2007; 408: 297–315.
 23. **Kulkarni NH, Onyia JE, Zeng QQ, et al.** Orally bioavailable GSK-3 α/β dual inhibitor increases markers of cellular differentiation *in vitro* and bone mass *in vivo*. *J Bone Min Res*. 2006; 21: 910–20.
 24. **Coghlan MP, Culbert AA, Cross DA, et al.** Selective small molecule inhibitors of glycogen synthase kinase-3 modulate glycogen metabolism and gene transcription. *Chem Biol*. 2000; 7: 793–803.
 25. **Wagman AS, Johnson KW, Bussiere DE.** Discovery and development of GSK3 inhibitors for the treatment of type 2 diabetes. *Curr Pharm Design*. 2004; 10: 1105–37.
 26. **Clevers H.** Wnt/ β -catenin signaling in development and disease. *Cell*. 2006; 127: 469–80.
 27. **Gebhardt R, Baldysiak-Figiel A, Krügel V, et al.** Hepatocellular expression of glutamine synthetase: an indicator of morphogen actions as master regulators of zonation in adult liver. *Prog Histochem Cytochem*. 2007; 41: 201–66.
 28. **Seidensticker MJ, Behrens.** Biochemical interactions in the wnt pathway. *J Biochim Biophys Acta*. 2000; 1495: 168–82.
 29. **Buillons LC, Levine AJ.** The role of β -catenin in cell adhesion, signal transduction, and cancer. *Curr Opin Oncol*. 1998; 10: 81–7.
 30. **Cadore A, Ovejero C, Saadi-Kheddouci S, et al.** Hepatomegaly in transgenic mice expressing an oncogenic form of β -catenin. *Cancer Res*. 2001; 61: 3245–49.
 31. **Thomas GM, Frame S, Goedert M, et al.** A GSK3-binding peptide from FRAT1 selectively inhibits the GSK3-catalysed phosphorylation of Axin and β -catenin. *FEBS Lett*. 1999; 458: 247–51.
 32. **Jope RS, Roh MS.** Glycogen synthase kinase-3 (GSK3) in psychiatric diseases and therapeutic interventions. *Curr Drug Targets*. 2006; 7: 1421–34.
 33. **Wodarz A, Nusse R.** Mechanisms of Wnt signaling in development. *Annu Rev Cell Dev Biol*. 1998; 14: 59–88.
 34. **Teich L, Daub KS, Krügel V, et al.** Synthesis and biological evaluation of new derivatives of emodin. *Bio Med Chem*. 2004; 12: 5961–71.
 35. **Yim H, Lee YH, Lee CH, et al.** Emodin, an anthraquinone derivative isolated from the rhizomes of *Eheum palmatum*, selectively inhibits the activity of casein kinase II as a competitive inhibitor. *Planta Med*. 1999; 65: 9–13.
 36. **Battistutta R, Sarno S, De Mliner E, et al.** The replacement of ATP by the competitive inhibitor emodin induces conformational modifications in the catalytic site of protein kinase CK2. *J Biol Chem*. 2000; 275: 29618–22.
 37. **Ding VW, Chen RH, McCormick F.** Differential regulation of glycogen synthase kinase 3 β by insulin and Wnt signaling. *J Biol Chem*. 2000; 275: 32475–81.
 38. **Schlupper D, Giesa S, Gebhardt R.** Influence of biotransformation of luteolin, luteolin 7-O-glucoside, 3',4'-dihydroxyflavone and apigenin by cultured rat hepatocytes on antioxidative capacity and inhibition of EGF receptor tyrosine kinase activity. *Planta Med*. 2006; 72: 596–603.
 39. **Gebhardt R, Hengstler J, Müller D, et al.** New hepatocyte *in vitro* systems for drug metabolism: metabolic capacity and recommendations for application in basic research and drug development, standard operation procedures. *Drug Metab. Rev*. 2003; 35: 145–213.
 40. **Burger HJ, Gebhardt R, Mayer C, et al.** Different capacities for amino acid transport in periportal and perivenous hepatocytes isolated by digitonin/collagenase perfusion. *Hepatology*. 1989; 9: 22–8.
 41. **Gebhardt R.** Antioxidative and protective properties of extracts from leaves of the artichoke (*Cynara scolymus* L.) against hydroperoxide-induced oxidative stress in cultured rat hepatocytes. *Toxicol Appl Pharmacol*. 1997; 144: 279–86.
 42. **Gebhardt R, Beck H.** Differential inhibitory effects of garlic-derived organosulfur compounds on cholesterol biosynthesis in primary rat hepatocyte cultures. *Lipids*. 1996; 31: 1269–76.
 43. **Fahrner J, Labruyere WT, Gaunitz C, et al.** Identification and functional characterization of regulatory elements of the glutamine synthetase gene from rat liver. *Eur J Biochem*. 1993; 213: 1067–73.
 44. **Kispert A, Vainio S, McMahon AP.** Wnt-4 is a mesenchymal signal for epithelial transformation of metanephric mesenchyme in the developing kidney. *Development*. 1998; 125: 4225–34.
 45. **Aoki M, Hecht A, Kruse U, et al.** Nuclear endpoint of Wnt signaling: neoplastic

- transformation induced by transactivating lymphoid-enhancing factor 1. *Proc Natl Acad Sci USA*. 1996; 96: 139–44.
46. **Snyder EY, Deitcher DL, Walsh C, et al.** Multipotent neural cell lines can engraft and participate in development of Mouse cerebellum. *Cell*. 1992; 68: 33–51.
 47. **Gaunitz F, Heise K.** HTS compatible assay for antioxidative agents using primary cultured hepatocytes. *Assay Drug Dev Technol*. 2003; 1: 469–77.
 48. **Cross DE, Watt PW, Shaw M, et al.** Insulin activates protein kinase B, inhibits glycogen synthase kinase-3 and activates glycogen synthase by rapamycin-insensitive pathways in skeletal muscle and adipose tissue. *FEBS Lett*. 1997; 406: 211–5.
 49. **Gebhardt R, Williams GM.** Amino acid transport in established adult rat liver epithelial cell lines. *Cell Biol Toxicol*. 1986; 2: 9–20.
 50. **Bradford MM.** A rapid and sensitive method for the quantitation of microgram quantities of protein utilizing the principle of protein-dye binding. *Anal. Biochem*. 1976; 72: 248–53.
 51. **Pfleiderer G.** Glykogen. Bestimmung als D-Glucose mit Hexokinase, Pyruvatkinase und Lactat-Dehydrogenase. In: Bergmeyer U, editor. *Methoden der enzymatischen analyse*. Weinheim: Verlag Chemie; 1962. pp. 59–62.
 52. **Haupt W, Gaunitz F, Gebhardt R.** Post-transcriptional inhibition of glutamine synthetase induction in rat liver epithelial cells exerted by conditioned medium from rat hepatocytes. *Life Sci*. 2000; 67: 3191–8.
 53. **Nagata Y, Hikada Y, Ishida F, et al.** Effect of simvastatin (MK-733) on the regulation of cholesterol synthesis in HepG2 cells. *Biochem Pharmacol*. 1990; 40: 843–50.
 54. **Aberle H, Schwartz H, Hoschuetzky H, et al.** Single amino acid substitutions in proteins of the armadillo gene family abolish their binding to alpha-catenin. *J Biol Chem*. 1996; 271:1520–6.
 55. **Hecht A, Litterst CM, Huber O, et al.** Functional characterization of multiple transactivating elements in beta-catenin, some of which interact with the TATA-binding protein *in vitro*. *J Biol Chem*. 1999; 274: 18017–25.
 56. **Austinat M, Dunsch R, Wittekind C, et al.** Correlation between beta-catenin mutations and expression of Wnt-signaling target genes in hepatocellular carcinoma. *Mol Cancer*. 2008; 7: 21.
 57. **Gaunitz F, Papke M.** Gene transfer and expression. *Methods Mol Biol*. 1998; 107: 361–70.
 58. **Bhat R, Xue Y, Berg S, et al.** Structural insights and biological effects of glycogen synthase kinase 3-specific inhibitor AR-A014418. *J Biol Chem*. 2003; 278: 45937–45.
 59. **Dewar MJS, Zoebisch EG, Healy EF, et al.** Development and use of quantum mechanical molecular models. 76. AM1: a new general purpose quantum mechanical molecular model. *J Am Chem Soc*. 1985; 107: 3902–9.
 60. **Morris GM, Goodsell DS, Halliday RS, et al.** Automated docking using a Lamarckian genetic algorithm and empirical binding free energy function. *J Comput Chem*. 1998; 19: 1639–62.
 61. **Jordan CT.** The leukemic stem cell. *Best Pract. Res. Clin. Haematol*. 2007; 20: 13–8.
 62. **Staal FJ, Noort M, Strous GJ, et al.** Wnt signals are transmitted through N-terminally dephosphorylated beta-catenin. *EMBO Rep*. 2002; 3: 63–8.
 63. **van Noort M, Meeldijk J, van der Zee R, et al.** Wnt signaling controls the phosphorylation status of beta-catenin. *J Biol Chem*. 2002; 277: 17901–5.
 64. **Hirsch C, Campano LM, Wöhrle S, et al.** Canonical Wnt signaling transiently stimulates proliferation and enhances neurogenesis in neonatal neural progenitor cultures. *Exp Cell Res*. 2007; 313: 572–87.
 65. **Aberle H, Bauer A, Stappert J, et al.** Beta-catenin is a target for the ubiquitin-proteasome pathway. *EMBO J*. 1997; 16: 3797–804.
 66. **Jho EH, Zhang T, Domon C, et al.** Wnt/beta-catenin/Tcf signaling induces the transcription of Axin2, a negative regulator of the signaling pathway. *Mol Cell Biol*. 2002; 22: 1172–83.
 67. **Leung JY, Kolligs FT, Wu R, et al.** Activation of AXIN2 expression by beta-catenin-T cell factor. A feedback repressor pathway regulating Wnt signaling. *J Biol Chem*. 2002; 277: 21657–65.
 68. **Lustig B, Jerchow B, Sachs M, et al.** Negative feedback loop of Wnt signaling through upregulation of conductin/axin2 in colorectal and liver tumors. *J Mol Cell Biol*. 2002; 22: 1184–93.
 69. **Loeppen S, Schneider D, Gaunitz F, et al.** Overexpression of glutamine synthetase is associated with beta-catenin-mutations in mouse liver tumors during promotion of hepatocarcinogenesis by phenobarbital. *Cancer Res*. 2002; 62: 5685–8.
 70. **Kruihof-de Julio M, Labruyère WT, Ruijter JM, et al.** The RL-ET-14 cell line mediates expression of glutamine synthetase through the upstream enhancer/promoter region. *J Hepatol*. 2005; 43: 126–31.
 71. **Hers I, Tavare JM, Denton RM.** The protein kinase C inhibitors bisindolylmaleimide I (GF 109203x) and IX (Ro 31–8220) are potent inhibitors of glycogen synthase kinase-3 activity. *FEBS Lett*. 1999; 460: 433–6.
 72. **Kuo GH, Prouty C, DeAngelis A, et al.** Synthesis and discovery of macrocyclic polyoxygenated Bis-7-azaindolylmaleimides as a novel series of potent and highly selective glycogen synthase kinase-3 beta inhibitors. *Med Chem*. 2002; 46: 4021–31.
 73. **Kunick K, Lauenroth K, Leost M, et al.** 1-Azakenpaullone is a selective inhibitor of glycogen synthase kinase-3 beta. *Bioorg Med Chem Lett*. 2004; 14: 413–6.
 74. **Logé C, Testard A, Thiéry V, et al.** Novel 9-oxo-thiazolo [5,4-f] quinazoline-2-carbonitrile derivatives as dual cyclin-dependent kinase 1 (CDK-1)/glycogen synthase kinase-3 (GSK-3) inhibitors: synthesis, biological evaluation and molecular modeling studies. *Eur J Med Chem*. 2008; 43: 1469–77. doi:10.1016/j.ejmech.2007.09.020.
 75. **Bertrand JA, Thieffine S, Vulpetti A, et al.** Structural characterization of the GSK-3beta active site using selective and non-selective ATP-mimetic inhibitors. *J Med Biol*. 2003; 333: 393–407.
 76. **Shin D, Lee SC, Heo YS, et al.** Design and synthesis of 7-hydroxy-1H-benzimidazole derivatives as novel inhibitors of glycogen synthase kinase-3beta. *Bioorg Med Chem Lett*. 2007; 17: 5686–9.
 77. **Xiao J, Guo Z, Guo Y, et al.** Inhibitory mode of N-phenyl-4-pyrazolo[1,5-b] pyridazin-3-ylpyrimidin-2-amine series derivatives against GSK-3: molecular docking and 3D-QSAR analyses. *Prot Eng Des Sel*. 2006; 19: 47–54.
 78. **Dessalew N, Bharatam PV.** Identification of potential glycogen kinase-3 inhibitors by structure based virtual screening. *Biophys Chem*. 2007; 128: 165–75.
 79. **Beurel E, Jope RS.** The paradoxical pro- and anti-apoptotic actions of GSK3 in the intrinsic and extrinsic apoptosis signaling pathways. *Prog Neurobiol*. 2006; 79: 173–89.

80. **Götschel F, Kern C, Lang S, et al.** Inhibition of GSK3 differentially modulates NF-kappaB, CREB, AP-1 and beta-catenin signaling in hepatocytes, but fails to promote TNF-alpha-induced apoptosis. *Exp Cell Res.* 2008; 314: 1351–66.
81. **Lefebvre V, Goffin I, Buc-Calderon P.** Fructose metabolism and cell survival in freshly isolated rat hepatocytes incubated under hypoxic conditions: proposals for potential clinical use. *Hepatology.* 1994; 20: 1567–76.
82. **Lochhead PA, Salt IP, Walker KS, et al.** 5-aminoimidazole-4-carboxamide riboside mimics the effects of insulin on the expression of the 2 key gluconeogenic genes PEPCK and glucose-6-phosphatase. *Diabetes.* 2000; 49: 896–903.
83. **Martinez A.** Preclinical efficacy on GSK-3 inhibitors: towards a future generation of powerful drugs. *Med Res Rev.* 2008; 28: 773–96. doi:10.1002/med.